

Numerical simulation of two-dimensional Rayleigh–Bénard convection in an enclosure

Nasreddine Ouertatani, Nader Ben Cheikh*, Brahim Ben Beya, Taieb Lili

Faculté des sciences de Tunis, département de physique, campus universitaire, 2092 El-Manar II, Tunisia

Received 6 December 2007; accepted after revision 1 February 2008

Available online 7 March 2008

Presented by Sébastien Candel

Abstract

In this Note, a numerical approach based on the finite volume method and a full multigrid acceleration is used, applied to the classical Rayleigh Bénard convection problem. Fine grids corresponding to 256^2 nodes are used and Benchmark solutions are proposed for Rayleigh numbers ranging from 10^3 to 10^6 . Some streamlines and isotherms are presented to analyze the natural convection flow patterns set up by the buoyancy force. **To cite this article:** *N. Ouertatani et al., C. R. Mecanique 336 (2008).*
© 2008 Académie des sciences. Published by Elsevier Masson SAS. All rights reserved.

Résumé

Simulation numérique bidimensionnelle d'une convection de type Rayleigh–Bénard dans une cavité carrée. La présente investigation porte sur une étude numérique bidimensionnelle relative à un problème de convection naturelle. Il s'agit en l'occurrence d'une convection de type Rayleigh Bénard dans une cavité carrée. Il est à noter qu'une convection de type Rayleigh Bénard peut être rencontrée dans de nombreuses applications physiques. On peut citer à titre d'exemple, le chauffage d'une pièce dans un immeuble ou encore le refroidissement de composants électroniques. Afin de correctement simuler l'écoulement, nous avons utilisé dans cette étude un maillage assez fin correspondant à 256^2 nœuds de calcul. La résolution numérique est basée sur une formulation de type volumes finis et une accélération multigrille. Des solutions Benchmark sont alors proposées relativement aux nombres de Rayleigh 10^3 , 10^4 , 10^5 et 10^6 . Une comparaison des résultats obtenus par la méthode classique RBSOR et la méthode multigrille est également faite et montre qu'un facteur gain de 17 peut être atteint. **Pour citer cet article :** *N. Ouertatani et al., C. R. Mecanique 336 (2008).*

© 2008 Académie des sciences. Published by Elsevier Masson SAS. All rights reserved.

Keywords: Heat transfer; Rayleigh–Bénard convection

Mots-clés : Transferts thermiques ; Convection Rayleigh–Bénard

* Corresponding author.

E-mail address: nader_bc@yahoo.fr (N. Ben Cheikh).

1. Introduction

Natural convection heat transfer in cavities has been a topic for many experimental and numerical studies found in the literature [1–3]. From practical and industrial point of views, the interest is justified by its many applications, which include heating and cooling of buildings, energy drying processes, solar energy collectors, etc. Most of the published works covering natural convection in enclosures that exist today can be classified into two groups: differentially heated enclosures [4–6] and enclosures heated from below and cooled from above (Rayleigh Bénard problems) [7–9]. Benchmark solutions related to differentially heated enclosures (first group) can be found in many numerical investigations [10–13]. However, numerical benchmark solutions related to the simplest case of 2D Rayleigh Bénard convection are less encountered in the literature. The Rayleigh Bénard convection is an important mechanism of mass and heat transfer in nature and in numerous industrial applications. One can cite geophysics, astrophysics, meteorology, heat exchangers, multilayer walls in buildings and cooling of electronic components for example. In addition to these applications, Rayleigh Bénard convection can also be studied to analyze fluid dynamic instability, bifurcation or chaotic behavior in fluids.

The aim of this Note is to propose two dimensional numerical solutions related to natural convection in a square enclosure heated from below and cooled from above. The fluid under consideration is air (Prandtl = 0.71) and the Rayleigh number is taken in the range $10^3 \leq Ra \leq 10^6$. Our numerical method is based on a finite volume formulation and an iterative Successive-Over-Relaxation scheme [18] with multigrid acceleration. The main idea of multigrid methods can be found in Refs. [21,22]. In this study, we have implemented our multigrid procedure in a so-called full multigrid (FMG) fashion [13]. Indeed, before starting V-cycles, the source term is calculated on the coarsest grid permitting the determination of an exact solution. This solution is progressively interpolated from the coarsest to the finest grid, used there as a starting guess for the V-cycle procedure. For more details about the method one can refer to [14]. In the present investigation, relatively fine grids corresponding to 256^2 nodes were used.

2. Mathematical formulation

A schematic representation of the system under investigation is shown in Fig. 1, where H is the dimension of the enclosure. The gravity vector is directed in the negative y coordinate direction, and the Boussinesq approximation is assumed to be valid.

The non-dimensional governing equations for the thermal convection problem are conservation of mass, the incompressible Navier–Stokes equations, and the energy equation:

$$\frac{\partial u_j}{\partial x_j} = 0 \tag{1}$$

$$\frac{\partial u_i}{\partial t} + \frac{\partial (u_i u_j)}{\partial x_j} = -\frac{\partial p}{\partial x_i} + \left(\frac{Pr}{Ra}\right)^{\frac{1}{2}} \frac{\partial^2 u_i}{\partial x_j \partial x_j} + \delta_{i2} \theta \tag{2}$$

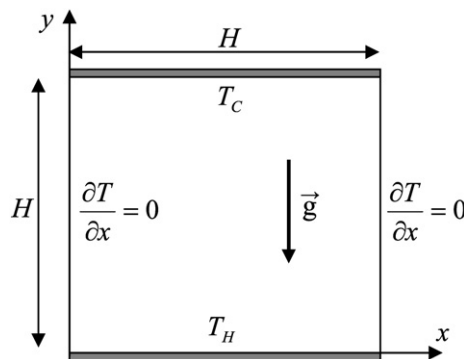


Fig. 1. Schematic diagram of the physical model and coordinate system.

Fig. 1. Schématisation du problème physique et système de coordonnées.

$$\frac{\partial \theta}{\partial t} + \frac{\partial(u_i \theta)}{\partial x_i} = (Ra Pr)^{-\frac{1}{2}} \frac{\partial^2 \theta}{\partial x_i \partial x_i} \quad (3)$$

where $u_i = (u, v)$, p , and θ are the velocity, the deviation from the hydrostatic pressure, and temperature, respectively; and δ_{ij} the Kröner symbol. These non-dimensional equations were obtained using the characteristic length H , velocity scale $u_0 = (g\beta H \Delta T)^{1/2}$, time scale $t_0 = H/u_0$, and pressure scale $p_0 = \rho u_0^2$. Here, ρ is the mass density, g the gravitational acceleration, and β the coefficient of thermal expansion. The non-dimensional temperature is defined in terms of the wall temperature difference and a reference temperature as:

$$\theta = \frac{T - T_r}{T_H - T_C} \quad \text{and} \quad T_r = \frac{1}{2}(T_H + T_C)$$

T_H is the temperature of the hot wall, and T_C is that of the cold wall. The Rayleigh number and Prandtl number are, respectively:

$$Ra = \frac{g\beta(T_H - T_C)H^3}{\alpha\nu} \quad \text{and} \quad Pr = \frac{\nu}{\alpha}$$

where α is the thermal diffusivity and ν the kinematic viscosity.

The enclosure boundary conditions consist of no-slip and no penetration walls, i.e., $u = v = 0$ on all four walls. The thermal boundary conditions on the bottom and top walls are:

$$\theta_{y=0} = \theta_H = +\frac{1}{2} \quad \text{and} \quad \theta_{y=1} = \theta_C = -\frac{1}{2}$$

The left and right vertical walls are adiabatic as shown in Fig. 1.

At each instant, the heat flux averaged over the hot wall is defined by:

$$Nu_H = - \int_0^1 \frac{\partial \theta}{\partial y} \Big|_{y=0} dx$$

3. Numerical methods

The unsteady Navier–Stokes and energy equations are discretized by a second-order time stepping of finite difference type. A projection method [15] is used to solve the Navier–Stokes equations. An intermediate velocity is first computed and later updated for satisfaction of mass continuity. In the intermediate velocity field the old pressure is used. A Poisson equation, with the divergence of the intermediate velocity field as the source term, is then solved to obtain the pressure correction and the real velocity field.

A finite-volume method [16] is used to discretize the Navier–Stokes and energy equations. The advective terms are discretized using a QUICK third-order scheme [17] in the momentum equation and a second order central differencing one in the energy equation.

The discretized momentum and energy equations are resolved using the red and black successive over relaxation method RBSOR [18], while the Poisson pressure correction equation is solved using a full multigrid method (FMG) [19]. The computational cost required to obtain the solution on different grids is reported in Table 1. The improvement factors in execution time, when comparing the single-grid RBSOR and multigrid algorithms, are of 3, 6.8, and 17.3 for grids 64^2 , 128^2 , and 256^2 , respectively. Other comparisons of the CPU performances of the numerical method related to an 8:1 differentially heated enclosure can be found in reference [23].

The convergence of the numerical results is established at each time step according to the following criterion:

$$\sqrt{\left(\sum_{i,j} X_{i,j}^k - \sum_{i,j} X_{i,j}^{k-1} \right)^2} \leq 10^{-7} \quad (4)$$

where X stands for u , v , p , or θ and k is the iteration level.

In order to ensure grid-independent solutions, a series of trial calculations for the case $Ra = 10^5$ and $Pr = 0.71$ were conducted for different non-uniform grid distributions, i.e., 32^2 , 64^2 , 128^2 and 256^2 . Table 2 shows the convergence

Table 1
CPU time performances obtained on a dual-core 1.73 GHz processor

Tableau 1
Performances des temps de calcul obtenues avec un processeur double-core à 1.73 GHz

Grid size	Time/step (RBSOR) [s]	Time/step (FMG) [s]	Improvement factor
64 × 64	0.09	0.03	3
128 × 128	0.96	0.14	6.8
256 × 256	15.39	0.89	17.3

Table 2
Convergence of u_{max} , v_{max} and Nu_H with grid refinement

Tableau 2
Convergence de u_{max} , v_{max} et Nu_H avec le raffinement des grilles

Grid size	u_{max}	v_{max}	Nu_H
32 × 32	0.3419	0.3714	3.8971
64 × 64	0.3438	0.3748	3.9072
128 × 128	0.3442	0.3756	3.9097
256 × 256	0.3443	0.3756	3.9103

Table 3
Comparison of our results with [20]

Tableau 3
Comparaison de nos résultats avec [20]

Grid size Ref. [20]	Nu_H Nu_C	Grid size Prés. study	Nu_H Nu_C
121 × 31	2.50326 2.50347	120 × 32	2.52664 2.52663
161 × 41	2.51604 2.51517	240 × 64	2.52668 2.52667
201 × 51	2.52234 2.52243	480 × 96	2.52523 2.52525

of the maximal values of velocity, (u_{max} , v_{max}), and the averaged Nusselt number, Nu_H , at the hot wall with grid refinement.

We then believe that the 256^2 grid is fine enough to get sufficient accurate solutions. Consequently, that grid was selected for all computations. Our numerical model was also checked for accuracy against the published numerical solution of C.Y. Soong et al. [20] for natural convection of air in a cavity of aspect ratio $A = 4$ heated from below. A comparison of the averaged Nusselt numbers Nu_H and Nu_C (through hot and cold walls respectively), are given in Table 3. As seen, our results are in quite good agreement with those of C.Y. Soong. Other validations of our numerical method were undertaken and gave excellent agreements (see Ref. [19]).

4. Results and discussion

All the results presented in this section are for $Pr = 0.71$. Computations are carried out for four different Rayleigh numbers, i.e. $Ra = 10^3$, 10^4 , 10^5 and 10^6 . A non-uniform grid with 256^2 nodes is selected for all computations. We believe that this grid is fine enough to get sufficient accurate solutions for $Ra \leq 10^6$.

Initially the fluid is considered at rest and the dimensionless temperature is taken equal to zero. The steady solution obtained for $Ra = 10^3$ was used as an initial one for the next Rayleigh number, and so on. Note that steady state was considered as achieved according to the following criterion:

$$\sum_{i,j} |X_{i,j}^{k+1} - X_{i,j}^k| \leq 10^{-5} \tag{5}$$

where X represents the variable u , v or θ , the superscript k refers to the iteration number and (i, j) refers to the space coordinates.

The horizontal and vertical velocity distributions at the mid-width ($x = 0.5$) and at the mid-height ($y = 0.5$) are presented in Figs. 2 and 3 respectively, for $10^4 \leq Ra \leq 10^6$.

As the velocity distribution indicates, the boundary layer is more closely confined to the walls with increase in the Rayleigh number. It is also observed that the velocity norm increases with the Rayleigh number meaning that convection dominates at high Ra .

The coordinate positions of the maximum x -velocity at the mid-plane $x = 0.5$ and the minimum y -velocity at the mid-height $y = 0.5$ can be depicted from Figs. 2 and 3 respectively and are reported in Table 4.

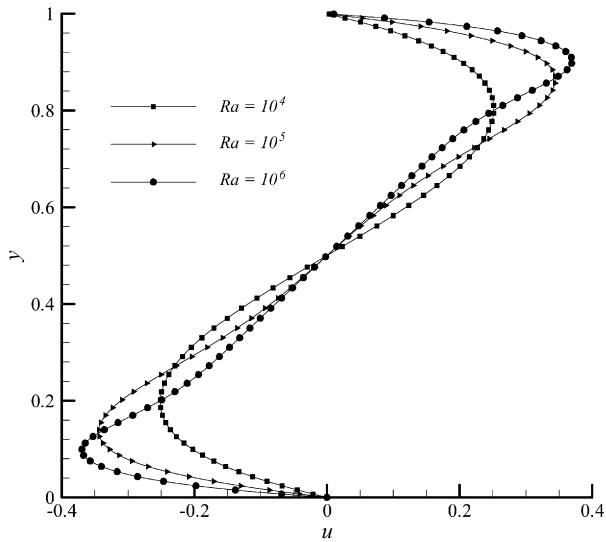


Fig. 2. Variation of horizontal velocity $u(y)$.
 Fig. 2. Variation de la vitesse horizontale $u(y)$.

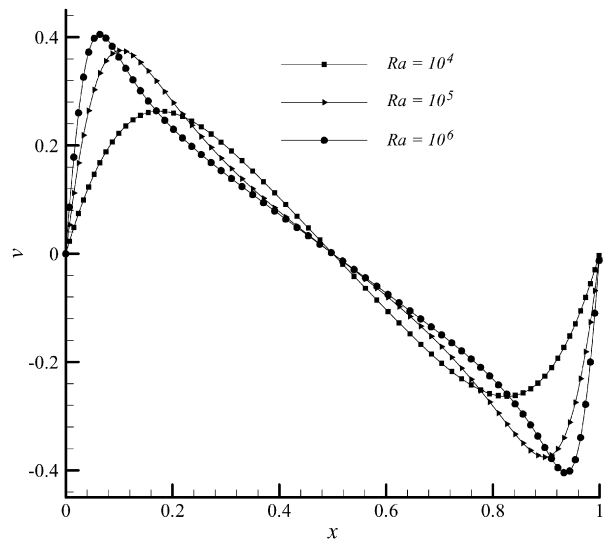


Fig. 3. Variation of vertical velocity $v(x)$.
 Fig. 3. Variation de la vitesse verticale $v(x)$.

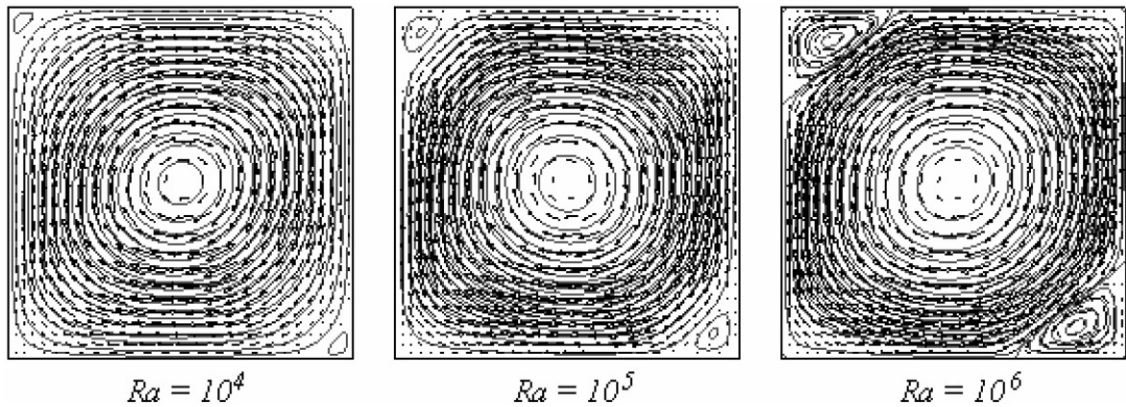


Fig. 4. Streamline contours for $Ra = 10^4, 10^5$ and 10^6 .
 Fig. 4. Allure des lignes de courant pour $Ra = 10^4, 10^5$ et 10^6 .

Streamlines and isotherms related to $Ra = 10^4, 10^5$ and 10^6 are reported in Figs. 4 and 5 respectively. For $Ra = 10^4$, the flow is symmetrical and is dominated by a recirculating motion in the core region. By increasing Ra , two secondary eddies are then observed at the top left and bottom right corners. The isotherms are also symmetrical and show the beginning of a convective motion for $Ra \geq 10^5$. The isotherm contours are indeed more distorted for $Ra \geq 10^5$.

As far as the heat transfer is considered, the local Nusselt number:

$$Nu = \left. \frac{\partial \theta}{\partial y} \right|_{y=0}$$

through the bottom hot wall as a function of the abscissa, is presented in Fig. 6. One can clearly see that the maximum heat transfer increases with the Rayleigh number. That maximum is localized at positions $x = 0.7183, x = 0.6993$ and $x = 0.6448$ for $Ra = 10^4, Ra = 10^5$ and $Ra = 10^6$ respectively. The corresponding maximum Nusselt values are then: $Nu_{\max}(Ra = 10^4) = 3.023, Nu_{\max}(Ra = 10^5) = 6.065$ and $Nu_{\max}(Ra = 10^6) = 11.69$.

Finally, we report in Table 5 our benchmark solutions obtained with our finite volume multigrid code. The table summarizes the mean Nusselt numbers Nu_H and Nu_C through the hot and the cold wall, respectively, and the maximal values of the horizontal and vertical velocity u_{\max} and v_{\max} for $Ra = 10^3, Ra = 10^4, Ra = 10^5$ and $Ra = 10^6$.

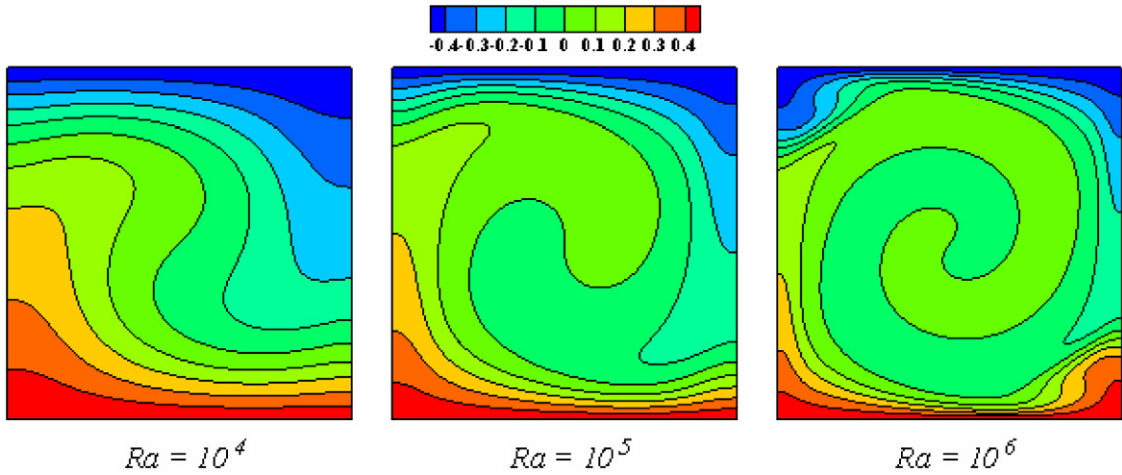


Fig. 5. Isotherm contours for $Ra = 10^4$, 10^5 and 10^6 .
 Fig. 5. Allure des isothermes pour $Ra = 10^4$, 10^5 et 10^6 .

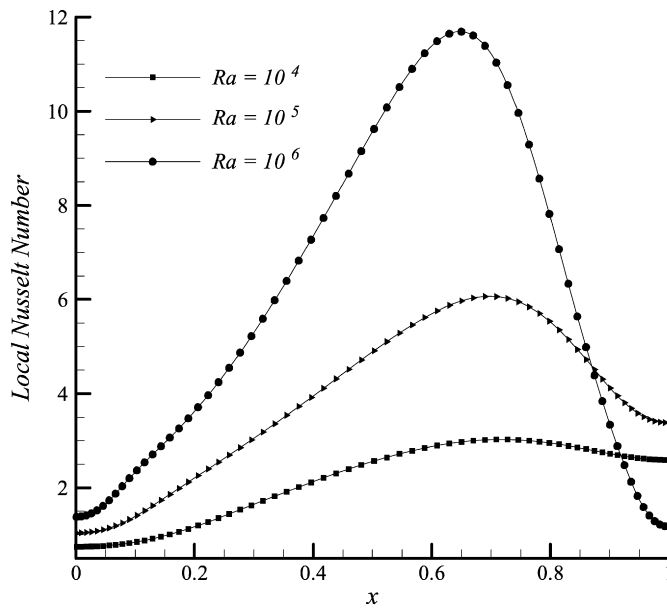


Fig. 6. Local Nusselt number through the hot wall.
 Fig. 6. Nombre de Nusselt local à travers la paroi chaude.

5. Conclusion

In this Note, a multigrid technique and a finite volume method were used to resolve the incompressible Navier–Stokes/Boussinesq equations. The code was applied to the classical two-dimensional Rayleigh Bénard convection problem in an enclosure with length-to-height aspect ratio $A = 1$ in which vertical walls were considered as insulated. A relatively fine grid corresponding to 256^2 nodes was selected to determine the problem Benchmark solutions. These solutions may be quite useful for validations of new numerical methods. Streamlines and isotherms were also presented in this paper to show the flow patterns for Rayleigh numbers ranging from 10^4 to 10^6 .

Table 4
Coordinate positions of u_{\max} and v_{\max}

Tableau 4 Coordonnées de u_{\max} et v_{\max}		
Rayleigh	$y(u_{\max})$	$x(v_{\max})$
10^4	0.8023	0.8263
10^5	0.8636	0.8973
10^6	0.9036	0.9359

Table 5
Benchmark solutions for $10^3 \leq Ra \leq 10^6$

Tableau 5 Solutions benchmark pour $10^3 \leq Ra \leq 10^6$				
Ra	Nu_H	Nu_C	u_{\max}	v_{\max}
10^3	1.0004	1.0004	3.6464×10^{-6}	3.9684×10^{-6}
10^4	2.1581	2.1580	0.25228	0.26369
10^5	3.9103	3.9103	0.34434	0.37569
10^6	6.3092	6.3092	0.37088	0.40600

References

- [1] A. Bejan, A.D. Kraus (Eds.), *Heat Transfer Handbook*, Wiley, New York, 2003.
- [2] D.B. Ingham, I. Pop (Eds.), *Transport Phenomena in Porous Media, II*, Pergamon, Oxford, 2002.
- [3] K. Vafai (Ed.), *Handbook of Porous Media*, Marcel Dekker, New York, 2000.
- [4] N.B. Cheikh, B.B. Beya, T. Lili, Aspect ratio effect on natural convection flow in a cavity submitted to a periodical temperature boundary, *J. Heat Transfer* 129 (2007) 1060–1068.
- [5] V.A.F. Costa, M.S.A. Oliveira, A.C.M. Sousa, Control of laminar natural convection in differentially heated square enclosures using solid inserts at the corners, *Int. J. Heat Mass Transfer* 46 (2003) 3529–3537.
- [6] G. Accary, I. Raspo, A 3D finite volume method for the prediction of a supercritical fluid buoyant flow in a differentially heated cavity, *Int. J. Heat Mass Transfer* 35 (2006) 1316–1331.
- [7] B. Calgagni, F. Marsili, M. Paroncini, Natural convective heat transfer in square enclosures heated from below, *Appl. Therm. Eng.* 25 (2005) 2522–2531.
- [8] J.K. Platten, M. Marcoux, A. Mojtabi, The Rayleigh–Bénard problem in extremely confined geometries with and without the Soret effect, *C. R. Mecanique* 335 (2007) 638–654.
- [9] F. Stella, E. Bucchigiani, Rayleigh–Bénard convection in limited domains: part 1 – oscillatory flow, *Numer. Heat Transfer A* 36 (1999) 1–16.
- [10] P. Le Quééré, Accurate solutions to the square thermally driven cavity at high Rayleigh number, *Comput. Fluids* 20 (1991) 29–41.
- [11] G. De Vahl Davis, Natural convection of air in a square cavity: a bench mark numerical solution, *Int. J. Numer. Methods Fluids* 3 (1983) 249–264.
- [12] S. Xin, P. Le Quééré, An extended Chebyshev pseudo-spectral benchmark for the differentially heated cavity, *Int. J. Numer. Methods Fluids* 40 (2002) 981–998.
- [13] M. Hortmann, M. Peric, G. Scheuerer, Finite volume multigrid prediction of laminar natural convection: bench-mark solutions, *Int. J. Numer. Methods Fluids* 11 (1990) 189–207.
- [14] N.B. Cheikh, B.B. Beya, T. Lili, Benchmark solution for time-dependent natural convection flows with an accelerated full-multigrid method, *Numer. Heat Transfer B* 52 (2007) 131–151.
- [15] Y. Achdou, J.L. Guermond, Convergence analysis of a finite element projection/Lagrange–Galerkin method for the incompressible Navier–Stokes equations, *SIAM J. Numer. Anal.* 37 (2000) 799–826.
- [16] S.V. Patankar, *Numerical Heat Transfer and Fluid Flow*, McGraw-Hill, New York, 1980.
- [17] B.P. Leonard, A stable and accurate convective modelling procedure based on quadratic upstream interpolation, *Comput. Meth. Appl. Mech. Eng.* 19 (1979) 59–98.
- [18] R. Barrett, et al., *Templates for the Solution of Linear Systems: Building Blocks for Iterative Methods*, SIAM, 1994.
- [19] E. Nobile, Simulation of time-dependent flow in cavities with the additive-correction multigrid method, Part I: Mathematical formulation, *Numer. Heat Transfer B* 30 (1996) 341–350.
- [20] C.Y. Soong, P.Y. Tzeng, D.C. Chiang, T.S. Sheu, Numerical study on mode-transition of natural convection in differentially heated inclined enclosures, *Int. J. Heat Mass Transfer* 39 (1996) 2869–2882.
- [21] W. Hackbusch, *Multigrid, Methods and Applications*, Springer-Verlag, Berlin/New York, 1985.
- [22] M. Hortmann, M. Peric, G. Scheuerer, Finite volume multigrid prediction of laminar natural convection: bench-mark solutions, *Int. J. Numer. Methods Fluids* 11 (1990) 189–207.
- [23] N.B. Cheikh, B.B. Beya, T. Lili, Natural convection flow in a tall enclosure using a multigrid method, *C. R. Mecanique* 335 (2007) 113–118.